Structural Material Property Tailoring of Dual Phase Titanium Alloy Microstructures Using Deep Neural Networks

Ryan Noraas,[1] Nagendra Somanath[2]
Pratt & Whitney Engines, United Technologies Corporation, East Hartford, CT 06108, USA

Michael Giering[3] Olusegun Oshin[4]
United Technologies Research Center, United Technologies Corporation, East Hartford, CT 06108, USA

I. ABSTRACT

Machine intelligence can enable businesses to improve performance by reducing errors and improving sensitivity, quality, speed, and in some cases achieving outcomes that go beyond current resource capabilities. The explosive increase in the power of numerical analytics combined with tensor algebra manifold optimization has been driven by breakthroughs in computational algorithms, machine learning and, to a large degree, deep neural networks (a.k.a. deep learning), enabling us to automate and learn from ever more complex datasets and engineer efficient rapid response algorithms in areas of practical relevance. These areas may include new product architecture design, rapid material characterization, life-cycle management and can be tied with a digital strategy that will enable efficient development from cradle to grave. Collectively, these technologies have been used to address fundamental challenges in materials engineering e.g. automated classification and quantification of microstructure images. In this work, a total of 19 different Ti-6Al-4V microstructures were produced by varying heat treat parameters such as solution temperature, cooling rate, aging times and temperatures. Over 14,000 images were collected and used to train models for microstructure classification, quantification, and synthetic image generation. A framework is proposed to enable rapid material design space exploration, property prediction and optimization that takes into account real-time decision cycles and trade-offs between speed and accuracy.

Keywords: Sensitivity, Deep Learning, Machine Learning, Optimization, MDO Algorithms, Physics, Processing,

II. NOMENCLATURE

W	=	width of image input (pixels)
H	=	height of image input (pixels)
D	=	depth (channels) of image input
A	=	Physics channel-physics property vector
P	=	Process Channel-processing parametric vector.

III. INTRODUCTION

Traditionally, the design methodology behind materials development has been very focused and isolated. It has been assumed that the toughest, lightest, strongest material would always be more beneficial to structural designers. Therefore, materials were developed independent of their intended use for optimal material performance rather than optimal structural performance or product application life cycle. This limited design philosophy often results in materials that over-perform in some macro level structural applications, resulting in higher costs, and under-perform in other situations, requiring the use of additional material and once again increasing cost. This inability of materials to meet proper multidisciplinary end

[1] Materials Engineer, Materials and Processes Engineering
[2] Principal Engineer, Systems Engineering and Optimization, Associate Fellow, AIAA.
[3] Technical Fellow, Research, Machine Intelligence
[4] Researcher, Autonomous and Intelligent Systems Department.

product performance objectives ultimately results in massive inflations in product costs in terms of economics, energy demand, and raw material resources.

Developing high performance materials requires control and understanding of composition, manufacturing process conditions, microstructure, as well as external factors such as environment and corrosion behavior Traditionally, ASTM specified controlled experiments are conducted to isolate the effect of one variable at a time. However, variables often are correlated with each other. It is infeasible to isolate some variable for experimental testing. Data mining can help reveal hidden relations between large amount of materials parameters, processing conditions and their relations with dependent materials properties. Traditional ways of material development can be disrupted and reshaped by making the use of available data.

Li and Fischer [1] proposed the integrated materials and structural design (ISMD) paradigm. This methodology links material scientists and engineers working on the micro-structural scale with structural designers working on the macro-structural scale through the design values which are common in both fields. Material engineers develop new materials for specific mechanical performance such as compressive strength, compliance or tensile ductility, and structural designers use these constitutive composite material properties in the design of structural members. By facilitating cooperation at this level between these two communities, materials can be engineered and tailored to closely match the expected structural demands, thus increasing the efficiency of the overall material-structure system. This is highly relevant in the harsh environment of high speed turbomachinery subject to high operational temperatures and pressures and diverse mechanical loads.

Bhadeshia et al. [2, 3] applied a neural network (NN) technique to model creep property and phase structure in steel. Crystal structure prediction and local crystal planes is another area of study for machine learning-based material identification due to the large amount of structural data in crystallographic databases using methods like K-nearest neighbor to identify localized material structure based on its nearest neighbors [4,5]. Machine learning is also applied for materials discovery by material constitutive composition, tailored constitutive design space for desired properties, which is essentially solving a constrained optimization problem. Rodemerck et al. [6] were able to find an effective multicomponent catalyst for low-temperature oxidation of low-concentration propane with a genetic algorithm and a neural network. Morgan and Ceder [7] identified the interdisciplinary nature of machine learning and recognized the challenges for developing methods needed for material tailoring at the micro-level, including predicting physiochemical properties of constituents, modeling electrical and mechanical properties, developing more effective catalysts, and predicting crystal structure. However, the inverse problem of identifying material properties based on constituents of the material is a more challenging *multidisciplinary optimization problem* because of the possibility of multiple solutions and the *enormous dimensionality* of the design space. Machine learning has shown promise in inverse materials discovery and design by rapid learning through deep neural networks and hence reducing the design space of relevance. Liu et al. [8] developed a machine learning method for the inverse design of Fe-Ge alloy microstructure with enhanced elastic, plastic and magnetostrictive properties. This method was validated with five design problems, which involves identification of microstructures that satisfy both linear and nonlinear property constraints. This framework shows supremacy comparing with traditional optimization methods in reducing as much as 80% of running time and achieving optimality that would be difficult or would not be attained.

Another more recent, data analytic approach to microstructure quantification is n-point spatial statistics. Spatial correlations (n=2) describe the first-order spatial correlations between the constituent distinct local states in the internal structure of the material [12]. Unlike traditional single point measures, n-point correlations account for the statistical and spatial arrangement of features in the microstructure. This added complexity comes at the expense of interpretability, where the spatial statistics are typically run through dimensional reduction algorithms to enable visualization of images in a low-dimensional latent space (2D

or 3D). Due to computational expense, the approach also generally requires upfront segmentation of images, which introduces additional bias as to what features are significant.

Convolutional neural networks (CNNs) are finding widespread adoption in the image domain and have enabled great strides in applications such as object detection, image classification and image segmentation [13]. Their success derives from the ability to make use of information at various length scales for pattern recognition. Many popular CNN architectures consist of three main types of differentiable layers: convolutional, pooling, and fully-connected (dense) [14-18]. Given enough data, CNNs are able to automatically learn scale-invariant critical features to enable image classification and quantification.

In many alloy systems, materials engineers and scientists may not know with certainty which features are relevant to a given material property e.g., grain size or precipitate volume fractions. In these cases, it can be of exceptional value to be able to automatically determine critical features in an image or materials microstructure, without the need for manual specification of said features. Using simplified parameters like average grain size may not numerically be adequate for prediction of complex material behavior. Higher order, spatial interactions (*N-point statistics*), color, or texture descriptors can all be captured using CNNs [11-18] and used to predict material phenomena with improved accuracy over simplified material descriptors. Specialized training techniques are required to minimize risk for over-fitting. Using a CNN model, it is possible to infer material pedigree robustly driven by thermomechanical processing parameters during manufacture, predict material properties, assess quality control (pass/fail), and detect outlier microstructures in an automatic fashion using images. The value of these models can be further realized if linked into the design phase or with an optimization engine that can discern location-specific properties and model-based material definition. Adoption of deep generative models such as augmented GANs may further enable materials design via generation of random, synthetic microstructure images for assessing effect of microstructural uncertainty on model predictions.

It is envisaged that linking of various deep convolutional and generative neural network-based models (CNN [14], GANs [15, 16], Autoencoders [17], Attention based models [18]) will enable a data-driven materials design/exploration approach using large historical databases built over time. If detailed material pedigree, properties, and microstructure images can be archived and made available to these machine learning models, benefits and sustained competitive advantage can be immediate.

The objective of this study are: [a] demonstrate the capacity of convolutional neural networks for microstructure classification and property prediction in Ti-6Al-4V, a workhorse alloy in the jet engine industry known for its high strength to weight ratio, low density, and exceptional corrosion resistance. [b] demonstrate the behavior of augmented GLOW models developed to perform classification of over 19 different heat treat pedigrees of the Ti-64 alloy, [c] demonstrate material design space exploration and the ability to predict high and low cycle fatigue,[d] Evaluate the use of deep generative models (conditional GANs, GLOW attention based). [e] Propose a deep learning based framework for linkage of various deep learning models and integration into an exploration/optimization design engine.

IV. PROBLEM FORMULATION

AUGMENTED MATRIX FORMULATION

Matrix augmentation describes the process of generating a constrained labeled matrix as part of the problem formulation using training data by transforming the given input training data by including the basic pixel image RGB channel data with the labeled data of measured attributes as an additional channel. Matrix data augmentation for deep learning is done to form a physics consistent formulation for optimization. Matrix data augmentation can be numerically beneficial as an additional regularizer for very deep architectures. It also allows for an easy way to incorporate known prior knowledge about image attributes, physics and

processing constraints. For example, if test images are taken with a varying amount of fatigue strength, it might make sense to augment with associated prior information of normalized fatigue strength.

SYNTHETIC DATA AUGMENTATION

Synthetic data augmentation describes a completely different approach to standard data augmentation. In this method, the input images are not transformed, but instead a generative model is tuned to generate additional, synthetic data resembling the real data. 2D models are used to render highly realistic images to increase amount of training data and improve the performance and predictability. Using GANs, it is possible to refine purely rendered data with information from real data to arrive at more realistic synthetic data. The standard GAN definition only allows for the generation of images, without respective labels. Therefore, for the generated data to be used for data augmentation, conventional GAN formulation needs to be modified to generate corresponding labels.

The main idea of our proposed embedded architecture is that we fuse the image and segmentation mask to create an image-segmentation pair. This is done by concatenating both images along the channel axis. As an example, a given RGB image of dimensions [W × H × 3] with its corresponding segmentation mask of dimensions [W × H × 1] results in an image segmentation pair with dimensions of [W ×H ×4]. When training the GAN, the generator is now modified to generate image-segmentation pairs, instead of just images. This change, in its most trivial form, can be achieved by simply modifying final convolutional layer in the generator, such that the number of output channels is equal to the number of channels of the required image-segmentation pair. For the discriminator, a similar principle is applied. The discriminator now takes image-segmentation pairs as input, and its goal is to correctly decide if any given image-segmentation pair is real or synthetic. Therefore, the first convolutional layer of the discriminator needs to be modified to accept inputs where the number of channels is equal to the number of channels of the image-segmentation pair (Figure 1).

Compared to the standard GAN formulation, this architectural adaptation is straight-forward to implement, as it is a simple change in the network architecture, and can therefore be used with any GAN training scheme, such as the Wasserstein Generative Adversarial Network (WGAN) or the more recent Wasserstein Generative Adversarial Network with Gradient Penalty (WGAN-GP).

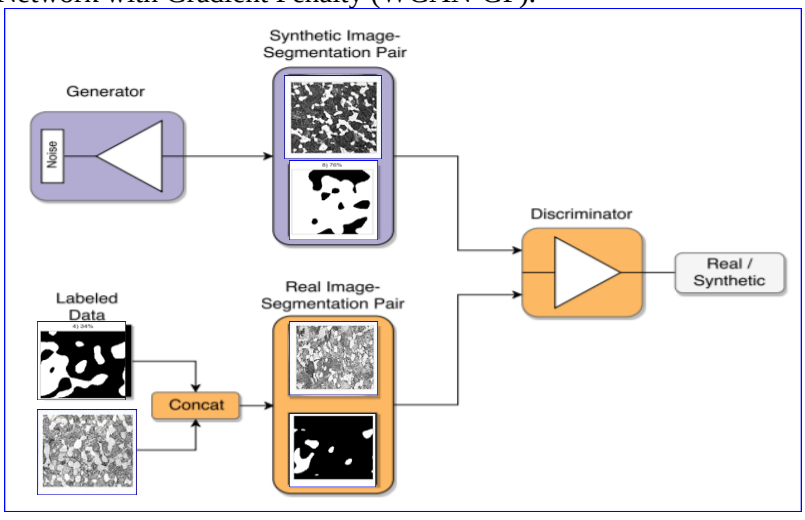

Figure1. Alloy Systems – Synthesis and Augmentation.

Similarity measures for image clusters and individual images generated by the network needs to be evaluated using standard metrics like the Dice Coefficient and the Hausdorff distance. The Sørenson-Dice coefficient [19, 20], referred to as the Dice coefficient or Dice score, is a metric for computing the similarity between two samples. It is computed as

$$DSC = \frac{2TP}{2TP + FP + FN}$$

Where, TP, FP and FN describe the true positives, false positives and false negatives between both samples, respectively. It can easily be applied to the problem of image segmentation, by simply computing a confusion matrix between predicted and labeled segmentation mask, and deriving the components of the Dice score from the confusion matrix.

The Hausdorff distance [21] measures the distance between two sets, by measuring how close each point of one set is to all points of the other set. The maximum distance (i.e. the farthest distance from a point in one set to its nearest neighbor in the other set) is the Hausdorff distance. It is defined as

$$H(A,B) = \max\big(h(A,B), h(B,A)\big)$$

Where,

$$h(A,B) = max_{a\in A} min_{b\in B} ||a - b||$$

is the directed Hausdorff distance, and ||a − b|| is a norm (e.g. the Euclidean norm) between point a from set A and point b from set B. Intuitively, the Hausdorff distance describes the most mismatched point between set A and set B, and therefore describes the largest distance between any points of A and B. Unlike the Dice and IoU, the Hausdorff distance has no explicit pairing of points, i.e. many points of A might be close to a single point of B

Conventional Microstructure Analysis: Microstructure analysis remains largely reliant on domain expertise, institutional knowledge, and visual conformity to established materials specifications. Calculation of grain sizes and phase fractions require the use of image analysis software. Repeatability and reproducibility is difficult due to variation in sample prep, imaging, and software. Current methods are not scalable to large datasets and predictive sensitivity has a large variation.

Convolutional Neural Networks (CNNs): The widespread adoption of neural networks in the image domain, has enabled great strides in object detection, image classification and image segmentation. Automatically learn spatial information and critical features at various length scales learning models and integration into an exploration/optimization design engine.

V. RESULTS

Ti-6Al-4V material micrograph images are surrounded by a padding band of black pixels. Measured attributes such as physical testing results for fatigue, creep, tensile stress etc., and processing parameters to encode them as colored patches within the padding band (Figure 2). Since there is only one set of such values per pedigree, the intra-class latent space learned by GLOW is consistent with the base model. The impact of the simultaneous modeling of the image and labels (attributes) on the inter-class latent space structure remains to be studied. Generative models ability to learn data-label pairs is one of their great strengths. Once trained, each point in the model latent space corresponds to an image-label pair. Our previous work demonstrated the validity of the microstructures synthesized in this manner [22]. This formulation allows us to simultaneously interpolate labels such as high-cycle fatigue for newly synthesized materials.

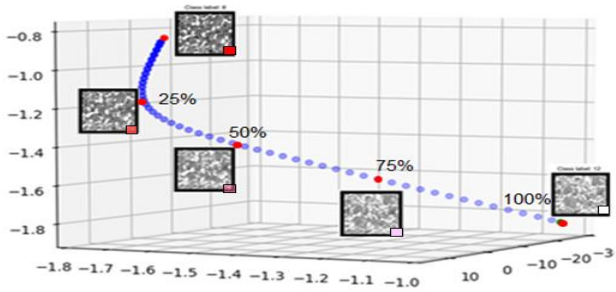

Synthesized microstructure image-label pairs generated by GLOW interpolation between actual image-label pairs in the latent manifold space.

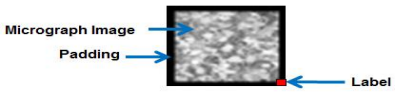

Image input to GLOW consists of a padded micrograph image and color patch to encode processing with physical test attribute information.

Figure 2. GLOW embedded material micrograph.

For our experiment our data set consists of 19 Ti-6Al-4V pedigrees where each pedigree differs only in processing attributes. The image dataset consists of 14,400 224x224 images evenly distributed across pedigrees and padded to 256x256 as shown in figure 2. A single experimentally determined value for the limiting high cycle fatigue for each pedigree is encoded as a patch on the image padding. [Train, test, validation] data sets were created by randomly sampling [70%, 20%, 10%] from each pedigree. The individual data sets identified are as follows:

DATA SETS:

1) <u>Microstructure Classification Dataset</u>: Size: 14,400 images (Ti-6Al-4V). Pedigree: 19 different heat treatments (varying solution temperature & cooling rates) – equal class balance.
Can a CNN match microstructure images to the corresponding heat treatment?
Modeling approach:

- Image feature extraction using pre-trained VGG16, followed by dimensionality reduction and training of logistic regression model.
- Fine-tune VGG16 on microstructure images and predict heat treat ID directly.
- Data was split 80/20 for training and validation.
- Real time data augmentation to reduce overfitting.

2) <u>Synthetic Two-Phase Dataset</u>: Size: 5,000 images (binary), Pedigree: White phase fraction ranging from 10-80%.
Can a CNN quantitatively predict phase fraction of white pixels in images?
Modeling approach:

- Modify VGG16 model by replacing soft-max classification layer with a dense layer of unit size to enable prediction of a single per training image. Also swap default 'categorical crossentropy' loss function for 'mean_squared_error'
- Data was split 80/20 for training and validation. Real-time data augmentation used to reduce overfitting.

<u>Alpha-beta Microstructures ("in the wild") Dataset</u>:

- Size: 2190 images (Ti-6Al-4V, Ti-6Al-2Sn-4Zr-2Mo)
- Pedigree: Various billet, bar, forging microstructures
- Problem statement: Can a CNN predict primary alpha volume fraction directly from images?

<u>Microstructure Classification</u>:

To determine the baseline performance for a simple image classification model, the microstructure images were run through a pre-trained VGG16 model and the output of the final dense layer was collected (4096 dimensional). Principal component analysis (PCA) was used to reduce dimensionality of the data prior to fitting a logistic regression model for image classification. The best classifier achieved a K-fold cross validation accuracy of 83% using 20 PCA components. To improve image classification accuracy, the VGG16 model was fine-tuned for microstructure images, and the model achieved a validation accuracy of 95% on 2800 images. This performance is used as a benchmark for comparison against improved GAN type models.

Microstructure Quantification:

All the prior work has focused on classification of microstructure images [22]. A natural extension of this work is to infer continuous value properties from image directly e.g. material properties or processing routes, without explicitly quantifying features and building response models [23]. Figure 3, shows quantitative predictions of pixel phase fraction on the synthetic validation (left) dataset (500 images), demonstrating good performance on new data. The CNN was then used to predict primary alpha volume fraction on real microstructure images (right). There is a strong correlation between measured and predicted results on both the training set (blue) and validation set (red). This data is used as benchmark for comparison against GAN-based approaches.

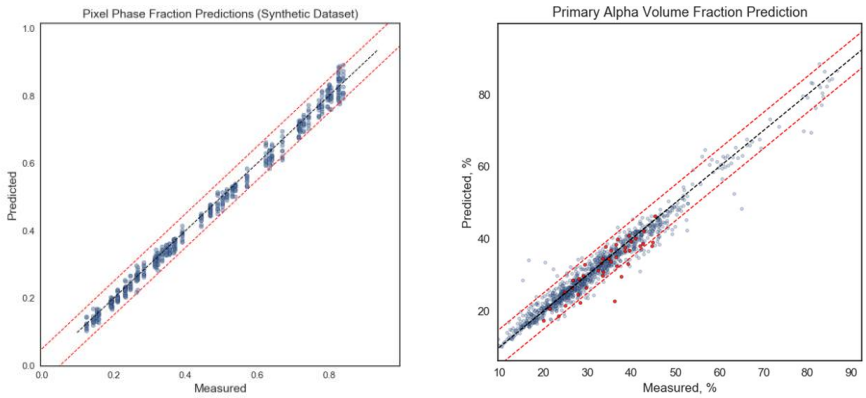

Figure 3. Alloy Systems – Pixel phase fraction for the synthetic validation.

During training of the GAN models, one of the 19 pedigrees was withheld from the model. From previous work [22] the withheld pedigree is expected to lie on a path between two other pedigrees. Interpolating along this path produces micrographs with physical characteristics that are indistinguishable from the pedigree held back. This suggests that the model is able to accurately interpolate between known pedigrees of material. In addition, using traditional methods for estimation of limiting HCF, generated images agree with the withheld ground truth values for HCF.

In this work physical test attributes of individual material alloy compositions are evaluated with the actual pixel information of the alloy composition of the alloy. Using the basic alloy compositions and its associated physics attributes, new alloy formulations and expected HCF attributes are arrived at using GLOW and CNN (VGG16) approaches.

Once a set of points P for a path connecting clusters, in the latent space is randomly chosen (see Figure 5). The latent space sampling gets anchored to it. The sampled points in the path can be reconstructed to evaluate microstructure image and associated predicted HCF value. Paths are an approach for random directed sampling from generative image models

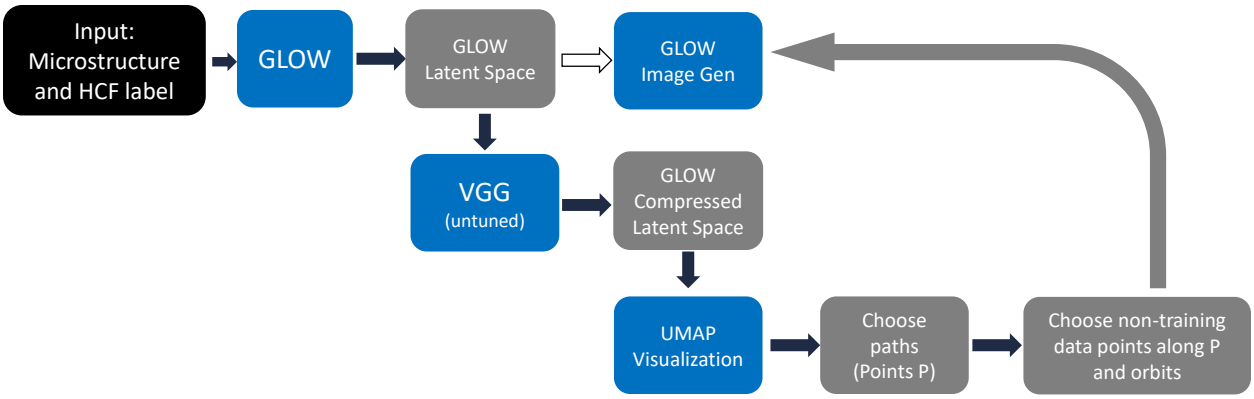

Figure 4. Alloy Systems Evaluation Flow.

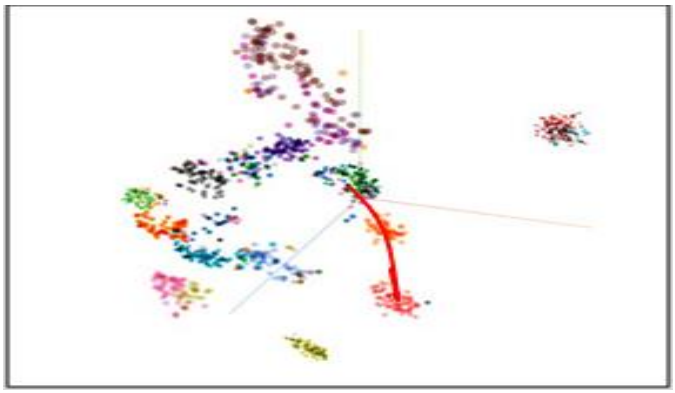

A sample path between through three alloy pedigrees (red). Withholding center cluster in training provides ground truth image-label pairs for validation.

Figure 5. Alloy Systems – Embedded space of 19 pedigrees.

The latent space of the GLOW model is high dimensional. Gaining intuition of positions of the relative locations of pedigree clusters in the latent space requires dimensional reduction and visualization. The UMAP visualization method [24] was chosen to ensure consistent repeatability of visualization and an ability to save and embed new data after training. It is confirmed that addition of the HCF information patch on the image did not noticeably impact the latent space. The latent space of the padded images is less separable, though relative cluster positions remain stable.

A VGG16 network [25] was tuned to predict the embedded pedigree class of microstructure alloys and normalized HCF data and then applied to GLOW generated image to see if it would be recognized as valid and of the correct class. GLOW generated micrographs were classified correctly 99% of the time along the path (precision=99%, recall = 95%). In the microstructure latent space orbital, GLOW model generates excellent microstructures. The garland-like artifact is a reflection of the offset bias.

The GLOW model was trained on 11 pedigrees for which high cycle fatigue data was available. In order to see how well microstructures are predicted for a material absent in training, one material pedigree (class 8) was removed during training of the GLOW model. Removing this pedigree disabled its ability to predict HCF in that region and degraded performance in areas that overlapped with it around index 300-500. This is evidence that the HCF predictions of this method aren't robust far outside of their training region.

Offsetting all points of the latent space to the mid-point between it and a neighboring data point results in new points having higher likelihood of being in the same class. The green line is the normalized HCF values across all 11 classes of the training data. The orange line shows the mean predicted HCF value after data was translated in the latent space. Aside from a bias term, the predicted HCF's are 99.4% correlated with the raw HCF's. Intra-class variance is small compared to the differences in the cluster HCF values.

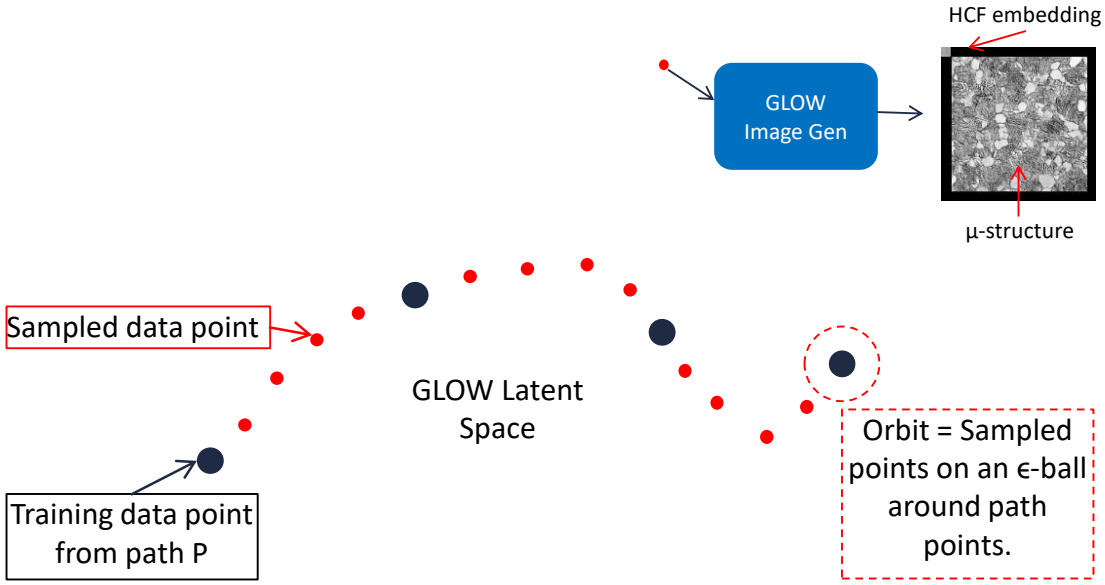

Figure 6. Inter-cluster Orbits

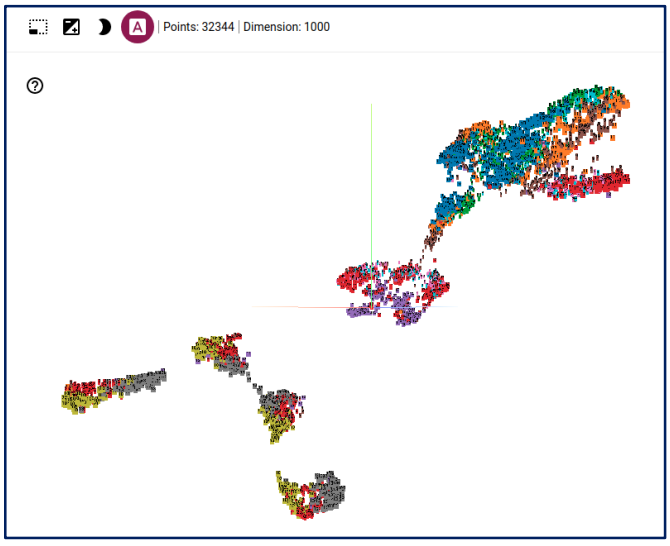

Figure 7. Intra-cluster UMAP visualization of design space.

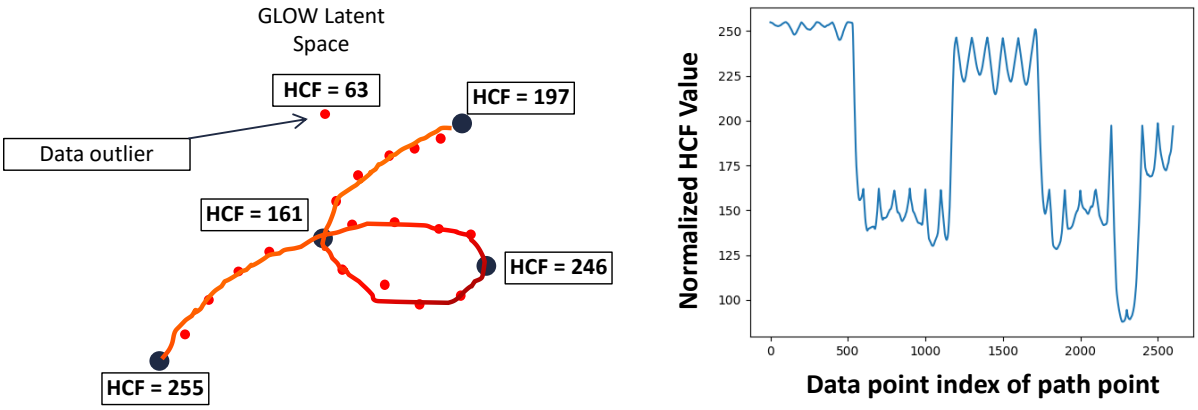

Figure 9. GLOW latent space and normalized HCF transition along traversed orbits.

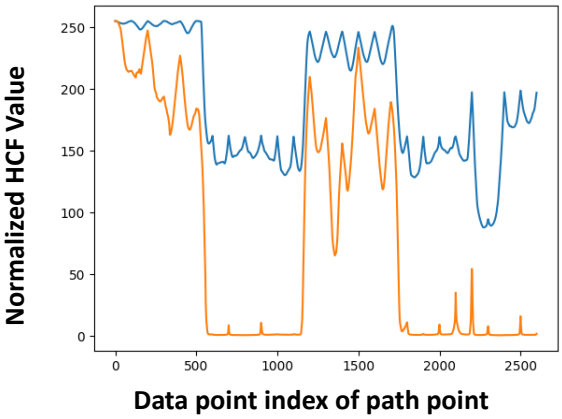

Figure 9. GLOW latent space and normalized HCF transition along traversed paths.

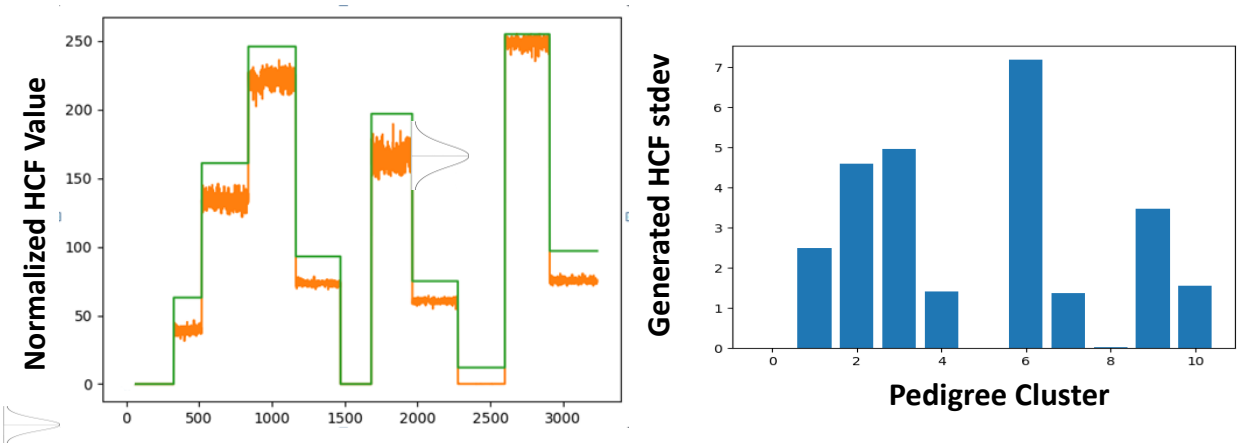

Figure 10. GLOW latent space and normalized HCF transition along traversed paths.

Validate Generated Microstructures: A VGG16 network was tuned to predict the pedigree class of the microstructure image dataset and applied to the GLOW generated images to see if they would be recognized

as valid and of correct class. The VGG classifier confusion matrix on real data performs well, aside from class 2, 3 which are difficult for even experts to discriminate. The precision and recall are both 93%. The results on the translated images had a precision of 63%and recall of 47%. Clearly, training for the HCF value and the microstructure simultaneously has degraded the generated microstructure image quality leading to poor classification results.

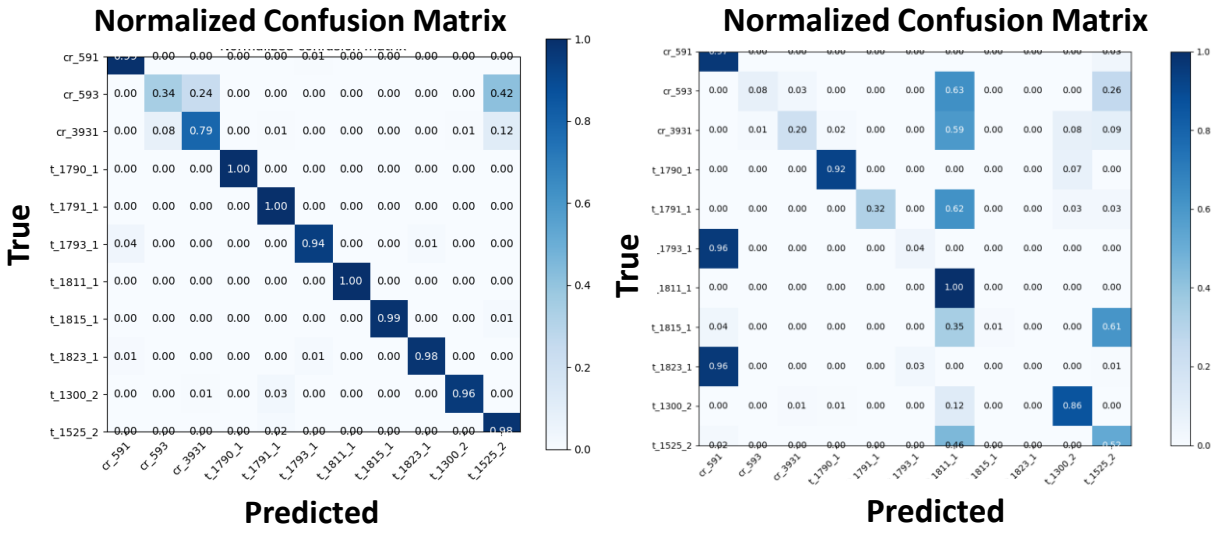

Figure 11. GLOW latent space and normalized HCF transition along traversed paths.

Conclusions

Convolutional neural networks (CNNs) were applied to various challenging problems in materials engineering such as image classification, quantitative property / image attribute prediction**,** and synthetic microstructure image generation. The models were shown to be able to accurately classify thousands of various Ti-6Al-4V microstructures, differentiated by heat treatment. The CNNs also demonstrated good performance in predicting quantitative attributes from images (phase fraction) –bypassing the need for image segmentation and analysis. Synthetic microstructures were generated using the GLOW model and were able to accurately classified by a CNN trained on real images. The GLOW model was then trained on a subset of the data (leave one out validation) in order to assess ability to interpolate between known pedigrees of material. The model had limited ability to predict HCF properties in the unknown region. Future work will include collection of additional microstructure images to further populate the sparse latent space and improve ability to interpolate between known pedigrees.

VI. ACKNOWLEDGEMENTS

The authors thank Pratt & Whitney and United Technologies Research Center for the support, including a cohesive and collaborative environment with sustained investment toward this work.

VII. REFERENCES

[1]. Li, V.C., and G. Fischer, "Reinforced ECC - An Evolution from Materials to Structures," *Proceedings of the First FIB Congress*, Osaka, Japan, Oct. 2002, pp.105-122.
[2]. Bhadeshia, H., "Design of Ferritic Creep-Resistant Steels," ISIJ, Int., 41, 626-640, 2001.
[3]. Sourmail, T., Bhadeshia, H., and MacKay, D.J.C., "Neural Network model of creep strength of austenitic stainless steels," Mater.Sci. Technol., 18, 655-663, 2002.
[4]. Bergerhoff, G., Hundt, R., Sievers, R., and Brown, I.D.," The inorganic crystal-structure data-base." J.Chem. Compu. Sci., 23. 66-69 1983.

[5]. White, P.S., Rodgers, J., and LePage, Y., "Crystmet: A Database of Structures and Powder Patterns of Metals and Intermetallics," Acta Cryst. B, 58, 343-348, 2002.
[6]. Rodemerck, U., Wolf, D., Buyevskaya, O.V., Claus, P., Senkan, S., and Baerns, M., "High-throughput synthesis and screening of catalytic materials-case study on the search for a low-temperature catalyst for the, oxidation of low-concentration propane." Chem. Eng. J., 82, 3-11, 2001.
[7]. Morgan, D. and Ceder, G., 2005. "Data mining in materials development", In *Handbook of Materials Modeling* (pp. 395-421). Springer, Dordrecht. 2005.
[8.] Liu, R., Kumar, A., Chen, Z., Agrawal, A., Sundararaghavan, V. and Choudhary, A., 2015. A predictive machine learning approach for microstructure optimization and materials design. *Scientific reports, 5*, p.11551.
[9]. Simonyan, K. and Zisserman, A., " Very deep convolutional networks for large-scale image Recognition", arXiv preprint arXiv:1409.1556. 2014.
[10]. Gatys, L., Ecker, A.S. and Bethge, M., "Texture synthesis using convolutional neural networks. In Advances in Neural Information Processing Systems*",* (pp. 262-270). 2015
[11]. Larsen, A.B.L, Sonderby, S, Larochelle, H. and Winther, O., "Autoencoding beyond pixels using a learned similarity metric", arXiv: 1512.09300v2 [cs.LG] 10 Feb 2016
[12]. Fullwood, W., Niezgoda, S., Kalidindi, S., "Microstructure reconstructions from 2-point statistics using phase-recovery algorithms", Acta Materialia 56(5):942:948, 2008.
[13]. Simonyan, K. and Zisserman, A., "Very deep convolutional networks for large-scale image Recognition", arXiv preprint arXiv: 1409.1556. 2014.
[14]. Gatys, L., Ecker, A.S. and Bethge, M., "Texture synthesis using convolutional neural networks. In Advances in Neural Information Processing Systems*",* (pp. 262-270). 2015
[15]. Lubbers, N., Lookman, T., Barros, K., "Inferring low-dimensional microstructure representations using convolutional neural networks", arXiv: 1611.02764v1. 2016
[16]. Larsen, A.B.L, Sonderby, S, Larochelle, H. and Winther, O., "Autoencoding beyond pixels using a learned similarity metric", arXiv: 1512.09300v2 [cs.LG] 10 Feb 2016
[17]. LeCun Y, Bengio Y., "Convolutional networks for images, speech, and time series", The Handbook of Brain Theory and Neural Networks. Apr; 3361(10):1995.
[18]. Erhan, D., Courville, A., and Bengio, Y., "Understanding representations learned in deep architectures. Department d'Informatique et Recherche Operationnelle, University of Montreal, QC, Canada, Tech. Rep, 1355, 2010.
[19]. Dice, L. R., "Measures of the amount of ecologic association between species", Ecology, 26(3):297–302, 1945.
[20]. Sørensen, T., "A method of establishing groups of equal amplitude in plant sociology based on similarity of species and its application to analyses of the vegetation on Danish commons", Biologiske Skrifter, 5:1–34,1948
[21]. Huttenlocher, D. P., Klanderman, G. A., and Rucklidge, W. A,"Comparing images using the Hausdorff distance. IEEE Transactions on Pattern Analysis and Machine Intelligence", 15(9):850–863, 1993.
[22]. Noraas, R, Nagendra, S., Giering,M, and Olusegun, O., "Structural Material Property Tailoring Using Deep Neural Networks", AIAA Scitech Meeting, SanDiego, Jan 7 – 10, 2019.
[23]. Noraas, R, Vasisht, V, Rettberg, L, Nagendra, S., Olusegun, O., Giering, M., "Recognition and Quantification of Dual Phase Titanium Alloy Microstructures Using Convolutional Neural Networks", Ti World Conference 2019, Location: Nantes, France, June 10-14th, 2019.
[24]. McInnes, L., Healy, J., Melville, J., "UMAP: Uniform Manifold Approximation and Projection for Dimension Reduction", arXiv:1802.03426v2 [stat.ML], December 6 2018.
[25]. Simonyan, Karen, and Andrew Zisserman. "Very deep convolutional networks for large-scale image recognition." arXiv preprint arXiv:1409.1556 (2014).